J Solid State Electrochem (2009) 13:1577–1584
DOI 10.1007/s10008-008-0732-y

ORIGINAL PAPER

# Silver electrodeposition from water–acetonitrile mixed solvents and mixed electrolytes in the presence of tetrabutylammonium perchlorate. Part I—electrochemical nucleation on glassy carbon electrode

**Claudio Mele · Sandra Rondinini · Lucia D'Urzo · Vincenzo Romanello · Elisabetta Tondo · Alessandro Minguzzi · Alberto Vertova · Benedetto Bozzini**

Received: 29 July 2008 / Revised: 4 November 2008 / Accepted: 4 November 2008 / Published online: 25 November 2008


**Abstract** Nucleation and growth of silver, electrodeposited from water–acetonitrile ($CH_3CN$ from 0 to 100% by volume) mixed solvents on glassy carbon electrodes, was studied by means of double-sweep voltammetry, current–time transients (CTT) and scanning electron microscopy (SEM). The effects of the addition of the specifically interacting tetrabuthylammonium cation were also investigated. From voltammetries, the formal potential, the nucleation potential and the cathodic current efficiency have been evaluated as a function of the mixed solvent composition. The key role on nucleation kinetics of transferring $Ag^+$ from the bulk phase to the $CH_3CN$-enriched electrode/solution interphase has been highlighted. CTT transients were described by a model combining instantaneous and progressive nucleation mechanisms. SEM images highlighted the effects of the presence of the organic solvent, which yields to a more regular growth, and of the quaternary ammonium salt, which exhibits grain-refining properties.

C. Mele (✉) · L. D'Urzo · V. Romanello · E. Tondo · B. Bozzini
Dipartimento di Ingegneria dell'Innovazione,
Salento University (formerly Lecce University),
via Monteroni,
73100 Lecce, Italy
e-mail: claudio.mele@unile.it

S. Rondinini · A. Minguzzi · A. Vertova
Department of Physical Chemistry and Electrochemistry,
University of Milan,
Via Golgi, 19,
20133 Milan, Italy

**Keywords** Mixed solvents · Silver · Acetonitrile · Tetrabutylammonium perchlorate

## Introduction

Electrodeposition of silver from cyanide solutions is a common industrial practice [1–3]. This kind of bath plating assures a high quality of the deposits, but is highly toxic. Thus, an extensive search has been made for satisfactory alternative electrolytes [4–6]. Silver electrodeposits prepared from $AgNO_3$ solutions prove to be very different from those obtained from cyanoalkaline baths and typically degenerate as dendrites [7–10]. The deposit quality can be improved with suitable additives, chiefly organic [4, 10]; nevertheless the standard of cyanoalkaline baths cannot be paralleled at the time of this writing. Despite their poor decorative quality, the studied deposits have larger surface areas and can be used as catalysts with interesting chemical, energetic and environmental applications.

Recently, the use of nonaqueous or mixed solvents gained a growing interest because they offer an alternative route for several electrochemical processes, allowing limited influence of water-related electrochemical reactions as well as the possibility of solubilising many organics [11, 12]. The study of the interfacial electrochemistry of $Ag/H_2O/CH_3CN$ systems has received some attention in the literature [13–15]. However, limited research effort has gone so far in the electrodeposition from nonaqueous phases [16–18]. In [19], a selection of nonaqueous-solvent based plating systems—specifically for iron-groups metals—has been reviewed. From electrodeposition and related literature, it results that

acetonitrile ($CH_3CN$) with quaternary ammonium salts as supporting electrolytes are promising electrolytes for metal electrodeposition [14, 18, 20].

Of course, nucleation and growth kinetics are critical for the understanding and control of the physicochemical properties of the electrodeposited materials [21–23]. The kinetics of the electrochemical nucleation of silver from aqueous solution on glassy carbon [22, 24] and other electrodes [25, 26] was extensively studied. Particular interest was devoted to the influence of temperature [24] and to rationalise the spatial distribution of nuclei [25]. The most frequently employed technique for these studies is the potential step method (see, e.g. [23, 27]). For mechanistic nucleation studies, different models were used, among which [22, 27–32].

Electrochemical nucleation studies of Ag in mixed solvents have not been published before to the best of the authors' knowledge. The selection of these systems for the present study stems from their prospective applications in electrocatalysis (e.g. [33–39]). Furthermore, the use of mixed solvents represents a new and exciting field of investigation for electrocrystallisation, with many important theoretical implications as well as potential technical and industrial applications. In the present paper, we study the nucleation of Ag onto glassy carbon electrode (GCE) by electrochemical methods (cyclic voltammetry and potentiostatic current transients) and the nucleation and growth morphology by scanning electron microscopy. Moreover, the effect of the addition of tetrabutylammonium perchlorate to mixed solvents was investigated.

## Experimental

The solutions used were $NaClO_4$ 0.1 M and $AgNO_3$ 10 mM with $CH_3CN$ in volume fractions varying from 0% to 100%. To this solution, tetrabutylammonium perchlorate (TBAP) 10 mM was added. The solutions were prepared with analytical grade chemicals supplied by Fluka and Aldrich, 99.8% HPLC-grade acetonitrile and ultra-pure water with 18.2 MΩ cm of resistivity from a Millipore-Milli-Q system.

Double-sweep voltammograms and current–time transients were recorded with a computer-controlled AMEL 5000 potentiostat. The working electrode was an AMEL 492/GC3 glassy carbon disk (3 mm diameter) embedded in a Teflon cylindrical holder. After each measurement, the glassy carbon was stripped chemically by immersion in concentrated $HNO_3$ and electrochemically by applying an anodic potential of +750 mV vs Ag/AgCl for a few minutes; an outstanding degree of reproducibility was obtained. A graphite bar with an exposed area of 7 $cm^2$ was used as counter electrode. The reference electrode was an AMEL Ag/AgCl containing a 3 M KCl separated from the electroplating solution by a porous ceramic interliquid junction. The reference electrode tip was placed at a distance ca. 5 mm from the working electrode. All potentials in this paper are reported vs Ag/AgCl for ease of reference. The voltammograms were recorded in the potential range +750 through −250 mV, with a scan rate of 10 mV $s^{-1}$.

The samples for scanning electron microscopy (SEM) were electrodeposited galvanostatically at −1 mA $cm^{-2}$ for 60 s from the solutions indicated above. The morphology of the samples was studied with a Cambridge Stereoscan 360 SEM. The electron source was $LaB_6$; the electron detection was carried out with a scintillation photodetector.

## Results and discussion

### Double-sweep voltammetry

In order to extract information on nucleation, the potential sweep was initiated at the anodic terminal voltage of +750 mV. For each bath, three replicate experiments were performed. The voltammetric behaviour of the Ag bath containing different percentages of $CH_3CN$, without and with TBAP, is shown in Figs. 1 and 2, respectively. In each voltammogram, two distinct voltammetric peaks, one during the negative going scan and one during the reverse scan, were clearly resolved. Silver deposition is evident by the appearance of a reduction peak in the range from +250 to +45 mV, the peak position depending on the percentage of $CH_3CN$. In the positive going scan, the stripping peak of

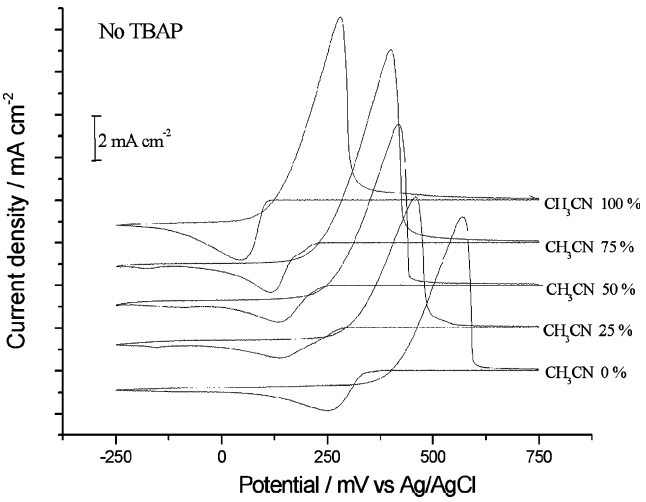


**Fig. 1** Double-sweep voltammograms for Ag electrodeposition from solutions containing $NaClO_4$ 0.1 M and $AgNO_3$ 10 mM, $CH_3CN$ in the volume fraction indicated. Working electrode: glassy carbon disk. Scan rate 10 mV $s^{-1}$

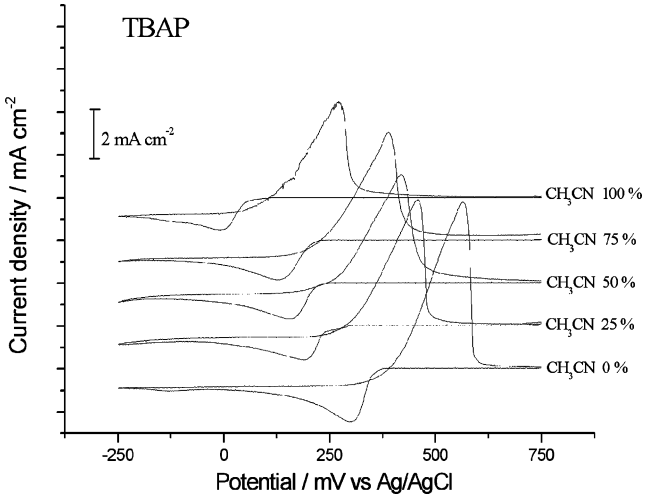


**Fig. 2** Double-sweep voltammograms for Ag electrodeposition from solutions containing $NaClO_4$ 0.1 M, $AgNO_3$ 10 mM and TBAP 10 mM, $CH_3CN$ in the volume fraction indicated. Working electrode: glassy carbon disk. Scan rate 10 mV $s^{-1}$

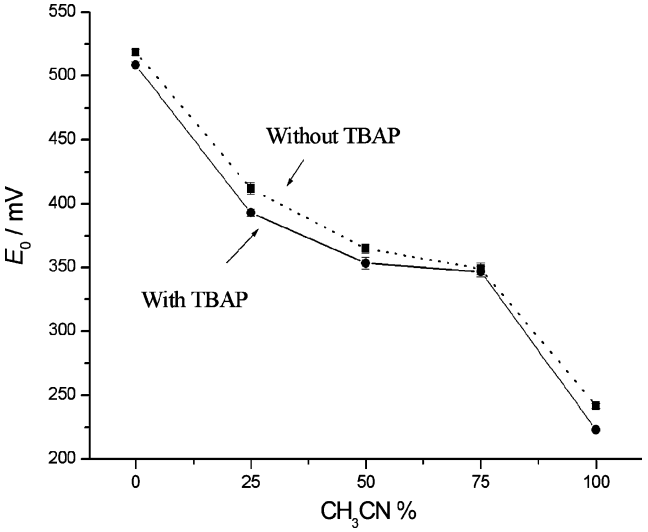


**Fig. 3** Formal potential ±1 SD, estimated from double-sweep voltammograms obtained on glassy carbon electrode from solutions containing $NaClO_4$ 0.1 M, $AgNO_3$ 10 mM, as a function of $CH_3CN$ percentage, without or with TBAP 10 mM. Scan rate 10 mV $s^{-1}$

the Ag previously deposited on the working electrode lies in the range from +570 to +280 mV, also in this case depending on the mixed solvent composition.

In Fig. 1, the voltammetric peaks appear bigger at higher percentage of $CH_3CN$. This fact can be explained as due to variation of mass transport in the different solutions. In fact, the viscosity of $CH_3CN$ is 38% of that of water, yielding a higher diffusion coefficient of silver. In the presence of TBAP (Fig. 2), smaller peaks are found, not depending on $CH_3CN$ content. This can be due to the increased viscosity of the solution due to the addition of TBAP [40].

In these voltammograms, a clear "cross over" of the anodic and the cathodic part of the cycle is noticed at potential $E_1$, denoting the presence of nucleation [23, 41, 42]. From these voltammograms, the formal potential $E_0$ (estimated from the potential under zero-current conditions, $E$), the nucleation overpotential $\eta_c$ (estimated as $\eta_c=E_1-E$) and the cathodic current efficiency have been evaluated for the silver electrodeposition baths with different amounts of $CH_3CN$.

A regular shift of $E_0$ towards more negative potentials is found upon increasing the percentage of $CH_3CN$, in both systems without and with TBAP (Fig. 3). The addition of TBAP to the solutions gives rise to a further shift of $E_0$ towards slightly more negative potentials. In Fig. 3, the mean values ±1 SD—estimated from the three replicate experiments—are reported.

The change of nucleation overpotential, $\eta_c$, upon varying the $CH_3CN$ volume fraction from 0 to 100%, is not monotonic, but a minimum can be observed at 75% and 50% for the system without and with TBAP, respectively (Fig. 4).

As far as the cathodic current efficiency is concerned both in the systems without and with TBAP, the value of this quantity has been found to increase systematically from ca. 65% to ca. 95% with the increase of the content of $CH_3CN$. The addition of the organic additive does not modify substantially the estimated values.

The shift in the $E_0$ value towards more negative potentials with the increase of $CH_3CN$% can be explained with the fact that, in the presence of $CH_3CN$, the surface

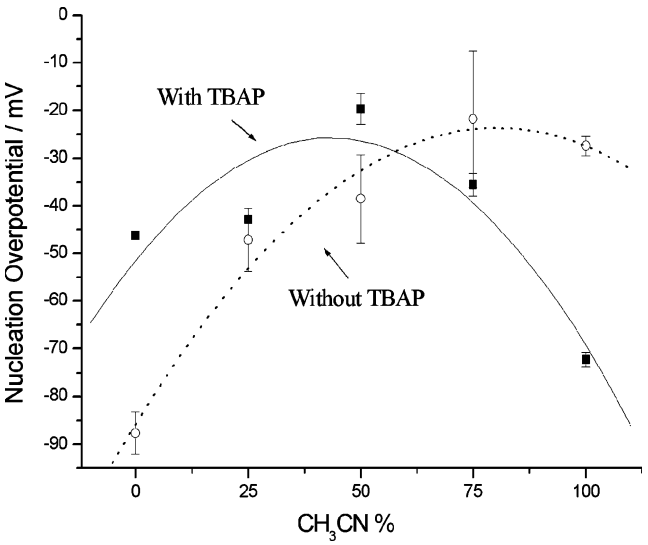


**Fig. 4** Nucleation overpotential ±1 SD, estimated from double-sweep voltammograms obtained on glassy carbon electrode from solutions containing $NaClO_4$ 0.1 M, $AgNO_3$ 10 mM, as a function of $CH_3CN$ percentage, without or with TBAP 10 mM. Scan rate 10 mV $s^{-1}$. Fitting lines obtained with the model reported in [11, 45] approximated to the second order

oxidation starts at less positive potentials than in the aqueous solutions [14]. According to the theory described in [11], in mixtures of water with solvents of lower Lewis basicity—such as $CH_3CN$—the organic component of the mixed solvent is preferentially adsorbed on the electrode, and the electrode surface may be largely covered by adsorbed organic molecules, even at relatively small concentrations of the organic solvent in the bulk. Therefore, the electrode surface layer will be preferentially populated by molecules of the organic solvent, while the reactant still contains water in its solvation shell. Transfer of silver from the solution phase to the metallic cluster can be described with the following model (Fig. 5):

$$Ag^{+}_{water+CH_3CN} \rightarrow Ag^{+}_{CH_3CN} \rightarrow Ag_{adatom} \rightarrow Ag_{cluster} \quad (1)$$

According to this model, elaborating on [43, 44], the Gibbs free energy of formation of a three-dimensional cluster consisting of $N$ atoms, with $N \geq 0$, as required by [43], can be given by:

$$\Delta G_{tot} = N\Delta G_{tr} - Nze\eta_c + \phi(N) \quad (2)$$

The first term accounts for the free energy of transfer [11] of $N$ $Ag^+$ cations from the bulk of the mixed solvent to the electrolyte in contact with the electrode that, at equilibrium, is composed of pure $CH_3CN$ [14]. The second term accounts for the transfer of the $N$ atoms across the double layer at the crystallisation overpotential $\eta_c$; the third term accounts for the increase of the surface energy due to creation of the surface of a cluster.

$$\phi(N) = S_{cs}(\sigma - \beta) + \sum_i \sigma_i S_i \quad (3)$$

where $\sigma$ is the specific surface energy, $\beta$ is the cluster–substrate interaction per unit contact area, and then, $S_{cs}(\sigma - \beta)$ is the surface free energy of the cluster–substrate interface and $\sum_i \sigma_i S_i$ is the surface free energy of the cluster–solution interface [44].

Assuming a hemispherical deposit having radius $A$, made up of $N$ atoms having radius $a$,

$$\phi(N) = \pi a^2 N^{\frac{2}{3}}(3\sigma - \beta) \quad (4)$$

So,

$$\Delta G_{tot} = N\Delta G_{tr} - Nze\eta_c + \pi a^2 N^{\frac{2}{3}}(3\sigma - \beta) \quad (5)$$

The maximum of $\Delta G(N)$ corresponds to the size of the critical nucleus $N_{cr}$, for $N > N_{cr}$ further growth of the cluster is connected with a decrease of the free energy and proceeds spontaneously. From Eq. 5, the nucleation overpotential $\eta_c$ can be written as:

$$\eta_c = \frac{1}{ze}\left(\Delta G_{tr} + \frac{2}{3}\frac{(3\sigma - \beta)\pi a^2}{\sqrt{[3]N}}\right) \quad (6)$$

As reported in [11] and in the references therein, the change of $\Delta G_{tr}$ with solvent composition typically has a maximum. Measuring $\Delta G_{tr}$ for the water–$CH_3CN$ system with added $AgNO_3$ is beyond the scope of this paper, but we conjecture that such a maximum exists also in this case on the basis of published data on water–$CH_3CN$ solutions in the same compositional range, with dissolved $Mn^{2+}$ [45]. Assuming the size of the critical nucleus a property of the material, then a maximum in $\Delta G_{tr}$ corresponds to a maximum in $\eta_c$. The experimental data can be fitted with the model reported in [11, 46] approximated to the second order. It is worth noting that Eqs. 2–6 contain purely thermodynamic information and that, in particular, ion transfer is treated according to the thermodynamic theory of Galus [11]. Furthermore, the electrode potential will depend on the activity of silver ions in the $CH_3CN$ layer, which, via $\Delta G_{tr}$, is of course also depending on the activity of silver ions in the mixed solvent bulk.

The systematic increase of the cathodic current efficiency is probably due to powder formation related to dendritic growth during the cathodic scan. Dendritic growth is in fact inhibited by $CH_3CN$ addition, as confirmed by SEM images

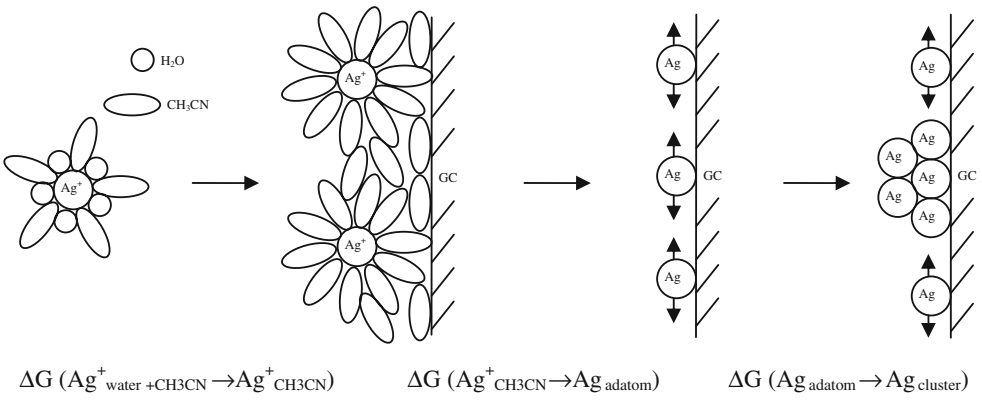


**Fig. 5** Sketch of the model adopted to describe the transfer of silver from the solution phase to the metallic cluster

reported in a following section, as well as by the presence of powder in the cell at the end of the voltammetric experiments.

## Current–time transients

CTTs were measured in order to study the Ag nucleation mechanism of the electrodeposition systems of interest onto GCE. Figure 6 shows a typical set of current transients (selected from our complete set of CTTs measured with different solvent compositions and overvoltages), recorded at different potentials for a content of $CH_3CN$ of 75%. The shape of the experimental current transients is similar to those described by many cognate experiments and predicted by several mathematical models based on mass transport as the rate determining step (e.g. [27, 29]). During the data elaboration, two probable causes of distorted results should be taken into account: a component of double-layer charging that dominates the initial part of the recorded data [23, 31] and instrumental limitations if the data-sampling rate is slower than the rate of current variations. The rising portion of our experimental transients is invariably in very good agreement with either instantaneous or progressive nucleation models, but the descending portion of the transients is generally higher than the one predicted by theory due to electrode roughening (Fig. 7).

In order to compare the electrodeposits obtained from mixed solvents of different composition, we adopted a simple purely phenomenological model (Eq. 9) based on one of the many available literature models that is compatible with our system. Equation 9 is meant as mere data description tool in terms of a single parameter. Among

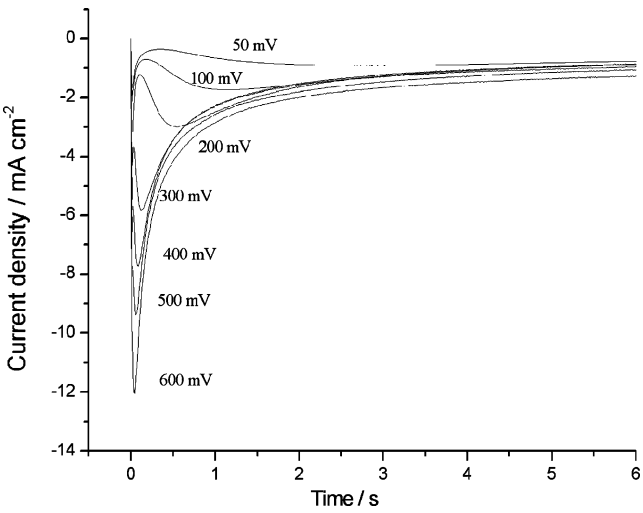


**Fig. 6** A set of experimental current density transients recorded in a solution containing $NaClO_4$ 0.1 M, $AgNO_3$ 10 mM and TBAP 10 mM, $CH_3CN$ in a volume fraction of 75%, for different overpotential step values indicated in the figure

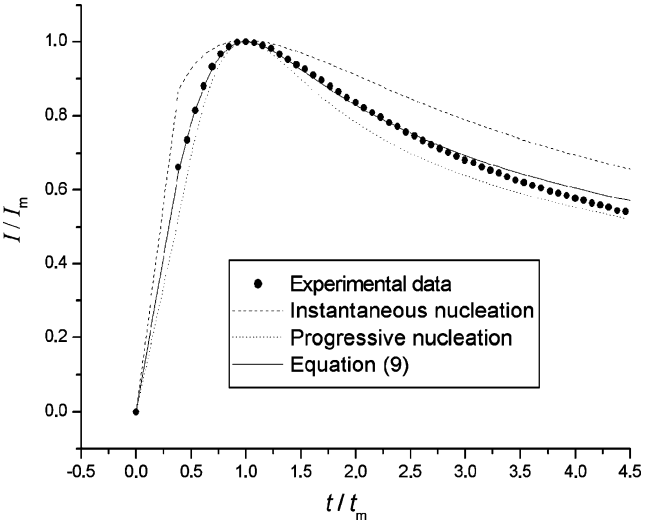


**Fig. 7** Nondimensional $I^2/I_m^2$ vs $t/t_m$ plots from potentiostatic nucleation transients. *Scatter* experimental data recorded during a potentiostatic current transients at $\eta_N$=−300 mV in a solution containing $NaClO_4$ 0.1 M, $AgNO_3$ 10 mM and TBAP 10 mM; $CH_3CN$ in a volume fraction of 75%. *Dashed line* instantaneous nucleation; *dotted line* progressive nucleation; *solid line* fitting of the experimental data using Eq. 9 (see text)

many essentially equivalent models [e.g. 27–32, 47–52], we chose those described in [27, 47] where the growth of nuclei is considered to be 3D, taking into account overlap of diffusion zones. For 3D nucleation with crystal growth controlled by localised hemispherical diffusion, the instantaneous and progressive nucleation types are described by the Eqs. 7 and 8. Normalised variables $i/i_m$ and $t/t_m$ are derived using experimental values for $i_m$ and $t_m$, the current and time at the current density maximum.

$$\frac{i^2}{i_m^2} = \frac{1.9452}{t/t_m}\left[1 - \exp\left(-1.2564\frac{t}{t_m}\right)\right]^2 \tag{7}$$

$$\frac{i^2}{i_m^2} = \frac{1.2254}{t/t_m}\left\{1 - \exp\left[-2.3367\left(\frac{t}{t_m}\right)^2\right]\right\}^2 \tag{8}$$

From the time behaviour of the transients and from the position of the current density maxima, the following conclusions can be drawn: (a) The transients are faster with the increase of the content of $CH_3CN$, and (b) the current density maximum of the transient is anticipated with the increase of the cathodic overvoltage. For comparison, the times corresponding to the current density maxima of the transients for solutions not containing TBAP are reported in Fig. 8. The same behaviour has been essentially found in the solutions with TBAP. Comparing the current

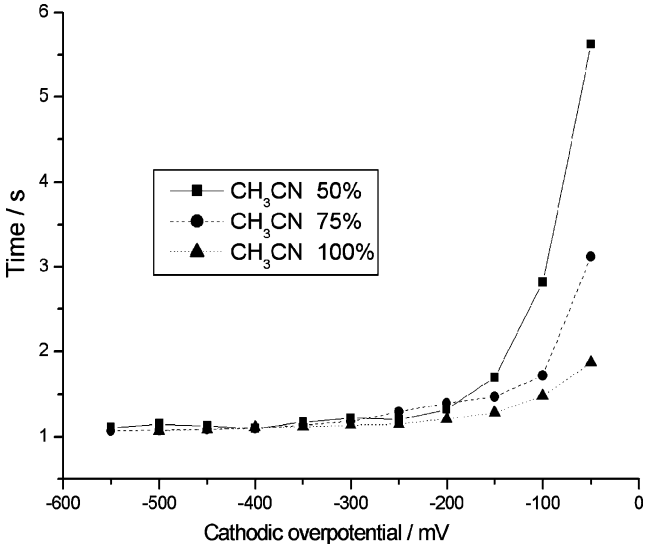


**Fig. 8** Time corresponding to the current density maxima estimated from potentiostatic transients recorded in a solution containing $NaClO_4$ 0.1 M and $AgNO_3$ 10 mM, without or with TBAP 10 mM, with the indicated $CH_3CN$%, as a function of the cathodic overpotential applied

peak of the transients (Fig. 9), higher values are observed upon increasing the $CH_3CN$% and by adding TBAP to the solutions, with particular effect for the solvents with higher $CH_3CN$%.

The nucleation mechanism has been evaluated using Eqs. 7 and 8. Indicating as $W$ the weight of instantaneous nucleation, the optimised nucleation mechanism has been estimated by combining Eqs. 7 and 8:

$$\frac{i^2}{i_m^2} = W\frac{1.9452}{t/t_m}\left[1-\exp\left(-1.2564\frac{t}{t_m}\right)\right]^2 + (1-W)\frac{1.2254}{t/t_m}\left\{1-\exp\left[-2.3367\left(\frac{t}{t_m}\right)^2\right]\right\}^2 \quad (9)$$

In the solutions with 100% of $CH_3CN$, only instantaneous nucleation can be observed in the investigated potential range. With mixed solvents, $W$ has been found to vary with $CH_3CN$% and potential. At lower overvoltages, the instantaneous nucleation mechanism is dominant, whereas at higher ones, the progressive mechanism prevails. With the increase of $CH_3CN$ content, the transition between instantaneous and progressive nucleation shifts towards more negative potentials. The threshold overpotential $\eta_{cr}$ results to be an exponential function of $x$, the $CH_3CN$ volume fraction, of the type:

$$\eta_{cr} = A + Be^{x/C} \quad (10)$$

where $\eta_{cr}$ is expressed in millivolts, $A$=165 mV, $B$=40 mV, $C$=0.44, and the linear correlation coefficient $\rho^2$=0.97. Then, $CH_3CN$ seems to hinder the progressive nucleation during the Ag electrodeposition process.

## Scanning electron microscopy of galvanostatic deposits

In-plane SEM micrographs of Ag layers deposited galvanostatically in the absence and in the presence of TBAP are shown in Fig. 10. The effects of organic solvent and surfactant are clearly visible: Upon increasing the $CH_3CN$ %, under the same electrochemical conditions, smaller nuclei and more compact deposits are obtained, the growth is more regular, and nucleation is partially inhibited; in fact, with the organic solvent, the surface density of nuclei seems to be reduced. Moreover, $CH_3CN$ hinders progressive nucleation, shifting the threshold from instantaneous to progressive nucleation towards more cathodic potentials. For 0% of $CH_3CN$, unstable growth and elongated crystallites appear; at 50% $CH_3CN$, an intermediate condition is found with crystallites that in some regions tend to cluster; at 100% $CH_3CN$, a globular grain structure made of small particles tends to dominate. This scenario is compatible with the electrochemical measurements reported in this work in terms of effects of solvent and quaternary ammonium salt on nucleation and growth mechanism. In particular, the presence of TBAP gives rise to remarkable grain refining as expected for cathodically adsorbed species. This point is also confirmed by Raman data, illustrated in a separate paper [53], where a higher degree of surface enhancement is observed in the experiments carried out in the presence of the quaternary ammonium salt, coherently with the generally accepted view of SERS effect

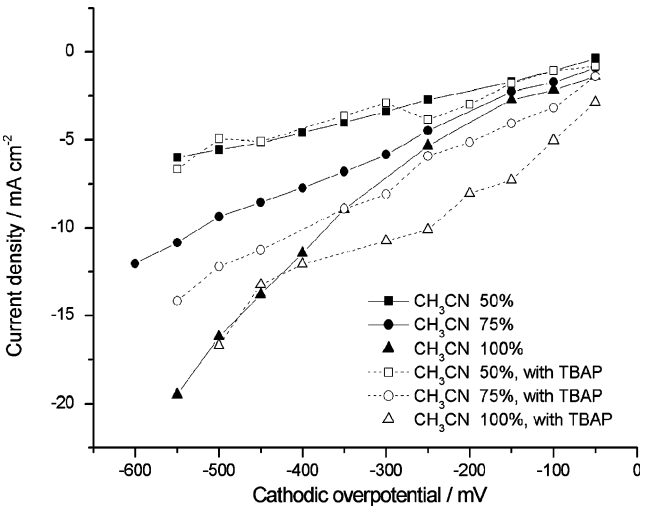


**Fig. 9** Current density maxima estimated from potentiostatic transients recorded in a solution containing $NaClO_4$ 0.1 M and $AgNO_3$ 10 mM, without or with TBAP 10 mM, with the indicated $CH_3CN$%, as a function of the cathodic overpotential applied

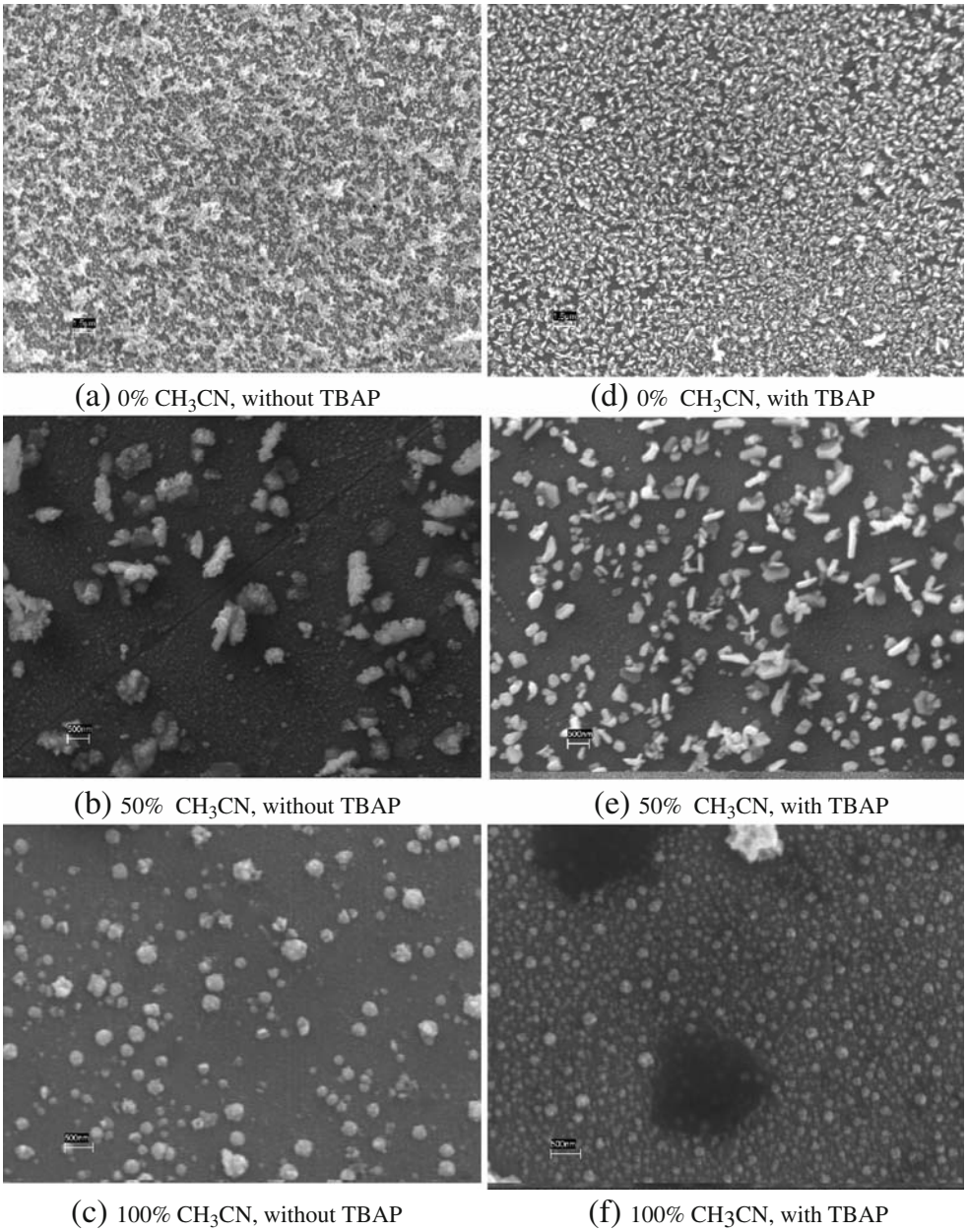


**Fig. 10** SEM micrographs of Ag deposited from solutions containing $NaClO_4$ 0.1 M, $AgNO_3$ 10 mM without (**a**, **b**, **c**) or with TBAP 10 mM (**d**, **e**, f), with the indicated $CH_3CN$%, obtained at −1 mA $cm^{-2}$ for 60 s. Magnification: **a**, **d** ×10,000; **b**, **e** ×20,000, **c**, **f** ×40,000

related to nanometric metal clusters present at the electrode surface [54].

## Conclusions

We studied Ag nucleation mechanisms during electrodeposition from aqueous–acetonitrile electrolytes in the presence of tetrabutylammonium perchlorate by electrochemical methods and SEM. Transfer of silver from the solution phase to the metallic one has been described with a model taking into account the fact that—in this system—the diffusion layer is preferentially populated by molecules of the organic component of the mixed solvent having a lower Lewis basicity. The contribution of instantaneous and progressive mechanisms has been estimated, and a transition overpotential between the two nucleation mechanism has been found, being a function of the molar fraction of acetonitrile. $CH_3CN$ has been proved to move the threshold from instantaneous to progressive nucleation towards more negative potentials. From SEM micrographs, a more regular growth of deposits can be observed upon increasing the $CH_3CN$%, and remarkable grain-refining effect was found for TBAP.

**Acknowledgements** Expert assistance with electrochemical experiments and SEM imaging of Mr. Francesco Bogani and Mr. Donato Cannoletta (University of Lecce), respectively, are gratefully acknowledged. Intensive assistance with data elaboration of Mr. Damiano Laveneziana is gratefully acknowledged. The financial support of MUR (FIRST funds) is gratefully acknowledged. Moreover, the authors wish to express their gratitude to one of the referees for some insightful suggestions and comments that called our attention on some interesting aspect of our experimental data—that we had initially overlooked—allowing us to produce a considerably improved manuscript.

## References

1. Elkington G, Elkington H (1840) Br Pat 8447
2. Dettke M (1991) Galvanotechnik 82:1238
3. Sadana YN, Wang SS, Wang ZZ (1988) Met Finish 86:37
4. de Oliveira GM, Barbosa LL, Broggi RL, Carlos IA (2005) J Electroanal Chem 578:151. doi:10.1016/j.jelechem.2004.12.033
5. Popov KI, Pavlovic MG, Grgur BN, Dimitrov AT, Hadzi Jordanov S (1998) J Appl Electrochem 28:797. doi:10.1023/A:1003450604118
6. Simon F, Kuhn W (2000) Galvanotechnik 91:2470
7. Evenepoel JC, Winand R (1970) Rev ATB Metab 10:132
8. Digard C, Maurin GR (1976) J Met Corros Ind 611:255
9. Vereeken J, Winand R (1976) J Electrochem Soc 123:643. doi:10.1149/1.2132902
10. Zarkadas GM, Stergiou A, Papanastasiou G (2001) J Appl Electrochem 31:1251. doi:10.1023/A:1012780022283
11. Galus Z (1995) In: Gerischer H, Tobias CW (eds) Advances in electrochemical science and engineering. VCH, Weinheim, pp 268–273
12. Chen R, Xu D, Gao G, Gui L (2004) Electrochim Acta 49:2243, doi:10.1016/j.electacta.2004.01.004
13. Cao P, Gu R, Qiu L, Sun R, Ren B, Tian Z (2003) Surf Sci 531:217. doi:10.1016/S0039-6028(03)00543-0
14. Doubova LM, Daolio S, Pagura C, De Battisti A, Trasatti S (2003) Russ J Electrochem 39(2):164. doi:10.1023/A:1022308925322
15. Gu R, Cao P, Sun YH, Tian Z (2002) J Electroanal Chem 528:121. doi:10.1016/S0022-0728(02)00898-7
16. Kuznetsov VV, Skibina LM, Loskutnikova IN (2000) Prot Metab 36(6):565. doi:10.1023/A:1026633312361
17. Kuznetsov VV, Skibina LM, Loskutnikova IN, Alekseev YE (2001) Prot Metab 37(1):31, doi:10.1023/A:1004881400861
18. Peng X, Xiang C, Xie Q, Kang Q, Yao S (2006) J Electroanal Chem 591:74. doi:10.1016/j.jelechem.2006.03.025
19. Watanabe T (2004) Nano-Plating. Elsevier, Tokyo
20. Ardizzone S, Cappelletti G, Mussini PR, Rondinini S, Doubova LM (2003) Russ J Electrochem 39(2):170. doi:10.1023/A:1022361009393
21. Paunovic M (1987) In: Romankiw LT, Turner DR (eds) Proc Symp Electrodeposition technology, theory and practice, vol 87-17. The Electrochemical Society, New York, p 345
22. Miranda-Hernández M, Palomar-Pardavé M, Batina N, González I (1998) J Electroanal Chem 443:81. doi:10.1016/S0022-0728(97)00487-7
23. Emery SB, Hubbley JL, Roy D (2004) J Electroanal Chem 568:121. doi:10.1016/j.jelechem.2004.01.012
24. Ramírez C, Arce EM, Romero-Romo M, Palomar-Pardavé M (2004) Solid State Ion 169:81. doi:10.1016/j.ssi.2004.01.023
25. Hyde ME, Jacobs RMJ, Compton RG (2004) J Electroanal Chem 562:61. doi:10.1016/j.jelechem.2003.08.009
26. Hernández N, Ortega JM, Choy M, Ortiz R (2001) J Electroanal Chem 515:123. doi:10.1016/S0022-0728(01)00619-2
27. Vargas T, Varma V (1991) In: Sarma R, Selman JR (Eds) Techniques for characterization of electrodes and electrochemical processes. Wiley, New York, pp 717–738
28. Palomar-Pardavé M, Ramírez MT, González I, Serruya A, Scharifker B (1998) J Electrochem Soc 143:1551. doi:10.1149/1.1836678
29. Scharifker B, Hills G (1983) Electrochim Acta 28:879. doi:10.1016/0013-4686(83)85163-9
30. Budevski E, Staikov GT, Lorenz WJ (1996) Electrochemical phase formation and growth. VCH, Weinheim
31. Grujicic D, Pesic B (2002) Electrochim Acta 47:2901. doi:10.1016/S0013-4686(02)00161-5
32. Palomar-Pardavé M, González I, Soto AB, Arce EM (1998) J Electroanal Chem 443:195. doi:10.1016/S0022-0728(97)00496-8
33. Rondinini S, Mussini PR, Specchia M, Vertova A (2001) J Electrochem Soc 148:D102, doi:10.1149/1.1379032
34. Fedurco M, Sartoretti CJ, Augustynski J (2001) Langmuir 17:2380. doi:10.1021/la0013751
35. Sonoyama N, Ezaki K, Fujii H, Sakata T (2002) Electrochim Acta 47:3847. doi:10.1016/S0013-4686(02)00324-9
36. Rondinini S, Vertova A (2004) Electrochim Acta 49:403. doi:10.1016/j.electacta.2003.12.061
37. Isse AA, Gottardello S, Maccato C, Gennaro A (2006) Electrochem Commun 8:1707. doi:10.1016/j.elecom.2006.08.001
38. Doherty AP, Koshechko V, Titov V, Mishura A (2007) J Electroanal Chem 602:91, doi:10.1016/j.jelechem.2006.12.004
39. Litster S, McLean G (2004) J Power Sources 130:61. doi:10.1016/j.jpowsour.2003.12.055
40. Kudryavtseva IV, Krumal'z BS, Mishchenko KP (1972) J Struct Chem 13:202. doi:10.1007/BF00744485
41. Fletcher S, Lwin T (1983) Electrochim Acta 28:237. doi:10.1016/0013-4686(83)85115-9
42. Fletcher S, Halliday CS, Gates D, Wescott M, Lwin T, Nelson G (1983) J Electroanal Chem 159:267. doi:10.1016/S0022-0728(83)80627-5
43. Budevski EB (1983) In: Conway BE, Bockris J'OM, Yeager E, Kahn SUM, White RE (eds) Comprehensive treatise of electrochemistry, vol 7, Kinetics and mechanism of electrode processes. Plenum, New York, p 410
44. Wong KP, Chan KC, Yue TM (2001) Appl Surf Sci 178:178. doi:10.1016/S0169-4332(01)00317-8
45. Broda J, Galus Z (1983) J Electroanal Chem 145:147. doi:10.1016/S0022-0728(83)80300-3
46. Covington AK, Newman KE (1979) Pure Appl Chem 51:2041. doi:10.1351/pac197951102041
47. Palomar-Pardavé M, Miranda-Hernández M, González I, Batina N (1998) Surf Sci 399:80. doi:10.1016/S0039-6028(97)00813-3
48. Heerman L, Tarallo A (1998) J Electroanal Chem 451:101. doi:10.1016/S0022-0728(98)00101-6
49. Heerman L, Tarallo A (1999) J Electroanal Chem 470:70, doi:10.1016/S0022-0728(99)00221-1
50. Milchev A, Heerman L (2003) Electrochim Acta 48:2903. doi:10.1016/S0013-4686(03)00355-4
51. Abyaneh MY (2006) J Electroanal Chem 586:196. doi:10.1016/j.jelechem.2005.10.004
52. Scharifker BR, Mostany J (1984) J Electroanal Chem 177:13. doi:10.1016/0022-0728(84)80207-7
53. Mele C, Bozzini B (2008) Silver electrodeposition from water–acetonitrile mixed solvents in the presence of tetrabutylammonium perchlorate. Part II—a SERS study of acetonitrile reactivity and tetrabutylammonium adsorption. J Solid State Electrochem doi:10.1007/s10008-008-0724-y
54. Lombardi JR, Birke RL (2008) J Phys Chem C 112:5605. doi:10.1021/jp800167v